PART SIX

TROLLEY WIRE MINE COMMUNICATIONS

PART SIX

TROLLEY WIRE MINE COMMUNICATIONS

TABLE OF CONTENTS

PART SIX

TROLLEY WIRE MINE COMMUNICATIONS

LIST OF FIGURES

PART SIX

TROLLEY WIRE MINE COMMUNICATIONS

LIST OF FIGURES
(Continued)

PART SIX

TROLLEY WIRE MINE COMMUNICATIONS

INTRODUCTION

This part of the final report treats some problems related to coal mine carrier frequency communication systems using the trolley wire/track transmission line. This work was undertaken for a brief period of time during the summer of 1972 to help understand, quantify, and improve some of the trolley wire carrier system behavior observed and/or predicted. Calculations and estimates of transmission line characteristic impedance, inductance and capacitance per unit length, mine motor loading effects, parallel line effects, and connection impedances are presented in Chapter I. Chapter II treats the design of r-f isolators for reducing the undesired and troublesome r-f loading that mine motors present to the trolley transmission line. Chapter III treats a diversity method for combatting standing wave nulls.

I. CALCULATIONS RELATED TO TROLLEY WIRE COMMUNICATIONS

A. ESTIMATION OF INDUCTANCE AND CAPACITANCE PER UNIT LENGTH OF TROLLEY LINES

To estimate the L and C per unit length of trolley lines, we use the eccentric line model of Section G of this Chapter, "Characteristic Impedance Estimates for Mine Trolley Lines." The capacitance per unit length for an eccentric line is given by (1)

$$C = \frac{2\pi\varepsilon}{\left[\cosh^{-1}\frac{m_2}{R_2} - \cosh^{-1}\frac{m_1'}{R_1'}\right]} \qquad (1)^*$$

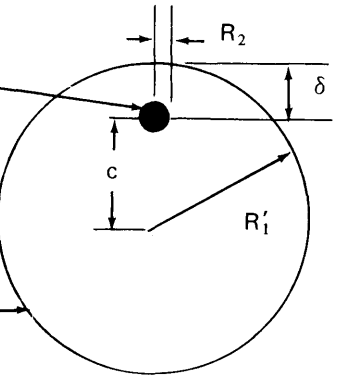

FIGURE 1 ECCENTRIC LINE MODEL OF TROLLEY LINE

where $m_1' = \frac{c}{2}\left[(\eta_1'^2 - \eta_2^2) + 1\right]$ (2)

$$m_2 = \frac{c}{2}\left[(\eta_1'^2 - \eta_2^2) - 1\right] \qquad (3)$$

$$\eta_1' = \frac{R_1'}{c}\,, \quad \eta_2 = \frac{R_2}{c}\,. \qquad (4a,b)$$

(1) E. Weber, Electromagnetic Fields, Theory and Applications, Vol. 1, 1957, pp. 119-121.

* References to Figures, Tables, and Equations apply to those in this Chapter unless otherwise noted.

The inductance per unit length can be obtained indirectly by substituting values for Z_o and C into the characteristic impedance expression.

$$Z_o = \sqrt{\frac{L}{C}} \quad . \tag{5}$$

The values for Z_o can be obtained from Figure 20, which were computed using the following equations[2]

$$Z_o = \frac{60}{\varepsilon^{1/2}} \cosh^{-1} U \tag{6}$$

$$U = 1/2 \, [D/d + d/D - 4c^2/dD] \tag{7}$$

$$c = \frac{D}{2} - \delta, \; \varepsilon = 1 \tag{8}$$

Substituting the appropriate values for high and low coal conditions, we get:

	High Coal	Low Coal
R_2	0.25"	0.25"
R_1'	36"	24"
δ	6"	3"
c	30"	21"
Z_o	230Ω	190Ω
C	15pf/m	18pf/m
L	0.8μh/m	0.65μh/m

B. EQUIVALENT CIRCUIT APPROXIMATION FOR THE TROLLEY POLE DROP WIRE TO MINE MOTORS

Using the eccentric transmission line model of Figure 1 which provides a good approximation to the trolley transmission line characteristic impedance, consider the effect of a vertical trolley pole wire to a motor, which is in turn connected to ground via the rails. Figure 2 depicts the trolley line

---

(2) ITT Reference Data for Radio Engineers, 5th Edition, Chapter 22, Transmission Lines, pp. 22-24.

and drop wire geometries, where the characteristic impedance is taken equal to 200 ohms and Z_m is the impedance of the motor at the trolley phone frequency.

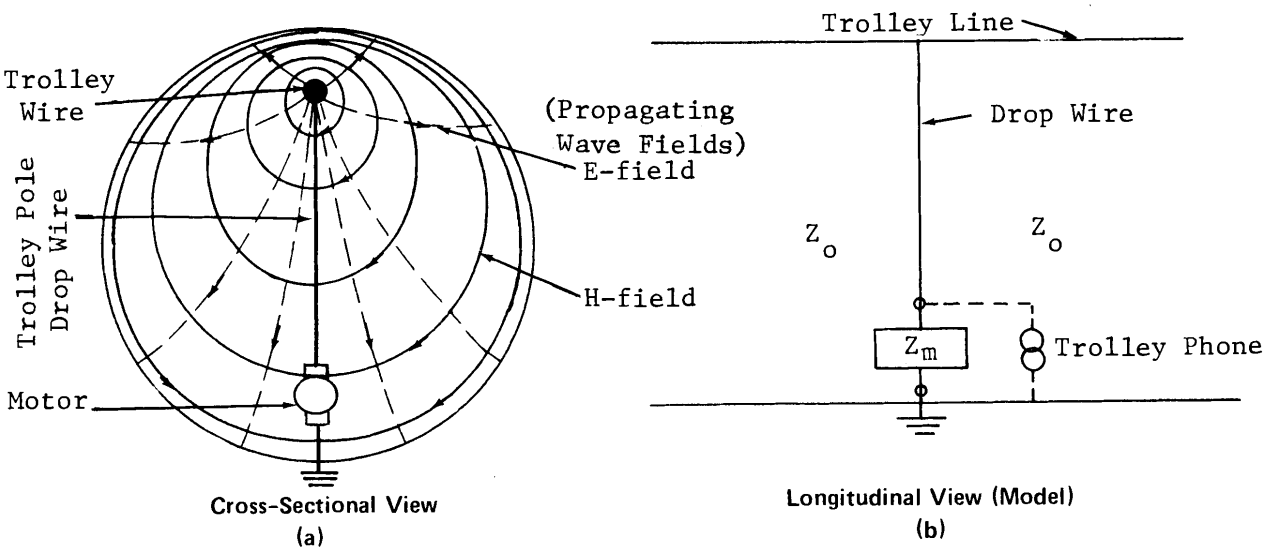

FIGURE 2 TROLLEY LINE MODEL

The trolley drop wire and low impedance motor do not represent a true or ideal short circuit in this situation, because the fields of a traveling wave are not prevented from coupling to the other side of the drop wire, as would be the case if the wire were replaced by a perfectly conducting plate across the whole haulageway cross-section. Therefore, the drop wire will allow energy to be inductively coupled between the sections of trolley line on each side of the drop wire, although this coupling will generally be weak.

Since the dimensions of the drop wire are small compared to a wavelength at 88kHz, it can be represented by a lumped inductance shunt element, L_s, as shown in Figure 3.

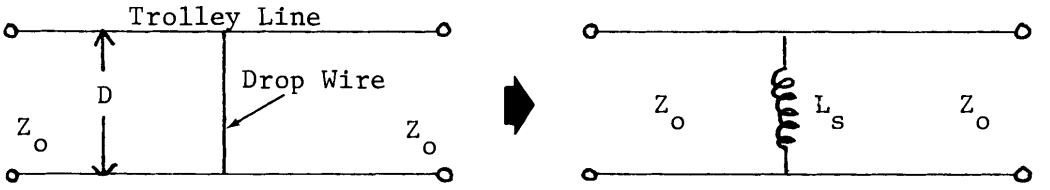

FIGURE 3 DROP WIRE AND EQUIVALENT SHUNT INDUCTANCE

The shunt inductance contribution L_s of the drop wire was estimated by computing the flux produced by the drop wire over the cross-sectional area $D_1 \times D_2$ shown in Figure 4.

$$\bar{H} = \bar{i}_\phi \frac{I}{2\pi r} \qquad (9)$$

$$\Phi = \int_o^{D_2} \int_o^{D_1} B \, da = L_s I \qquad (10)$$

$$L_s \cong \frac{\mu_o}{2\pi} D_1 \, \ell n \left(\frac{D_2}{a}\right) \qquad (11)$$

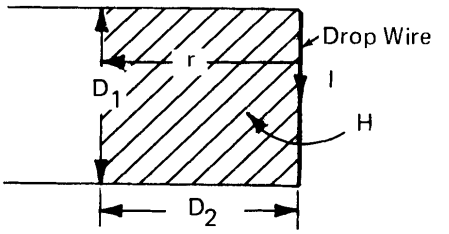

FIGURE 4 GEOMETRY FOR DROP WIRE

where a is the wire radius.

Letting a = 0.25 inches, and $D_2 = D_1 = 5.5$ feet for high coal and 4 feet for low coal, we get

	L_s	X_{L_s}
for high coal	1.9μh	1.1Ω
for low coal	1.3μh	0.75Ω

where X_{L_s} is the associated inductive reactance at 88 kHz (shown in Figure 5).

By comparison with these values of shunt reactance, the characteristic impedance of the trolley line $Z_o \cong 200$ ohms, the trolley phone impedance Z_T is a nominal 25 ohms, and the magnitude of the impedance Z_m of the motor in series with the drop wire is alleged to be on the order of 0.5 ohm when hauling at nominal speed. More measurements of the impedance behavior of typical locomotive motors at the trolley phone frequencies of 88 and 100 kHz are needed to confirm this reputed low impedance behavior and to determine whether it is representative for different motor installations on locomotives.

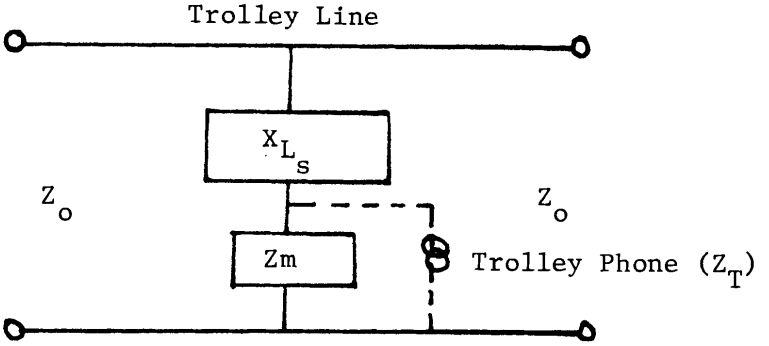

FIGURE 5 TROLLEY LINE AND ASSOCIATED IMPEDANCES

C. IMPEDANCE SEEN BY TROLLEY PHONES DUE TO CONNECTION METHOD

The trolley phones are presently coupled to the trolley line by connecting them in parallel with the low impedance trolley motors. The connections are made relatively close to the motor terminals so that little or no advantage is taken of any increase in impedance offered by the trolley pole drop wire inductance. Figure 6 illustrates typical geometry (6a) and an approximate equivalent circuit (6b).

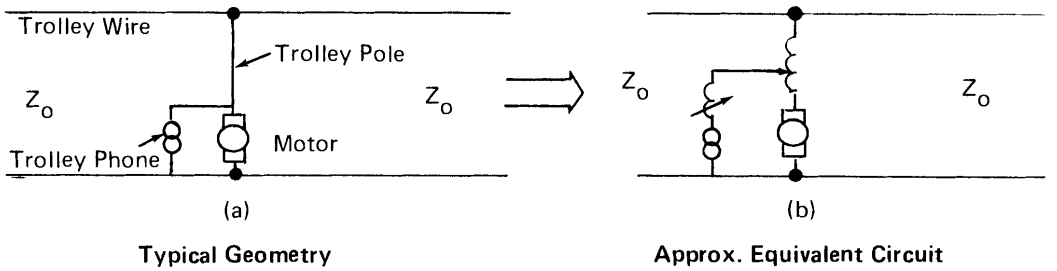

FIGURE 6 TROLLEY PHONE CONNECTION TO TROLLEY WIRE

Since the trolley motor impedance at 88kHz is reported to be on the order of 0.5 ohms, the motors will shunt most of the trolley signal away from the trolley line. By making the connection further up the drop wire, the shunt impedance presented by the motor can be increased by the drop wire inductive reactance. The objective of this section is to provide an estimate of the magnitude of this potential increase in impedance.

To estimate the shunt and series impedance for two different connections, the geometries of Figure 7 for the case of high coal were used.

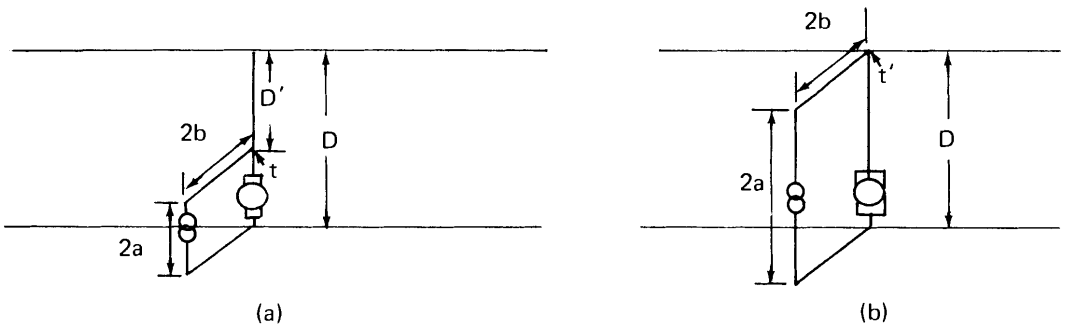

FIGURE 7 MODEL GEOMETRIES

Figure 7a approximates the present connection, t, while Figure 7b approximates a connection, t', to the top of the trolley pole. As seen from the trolley phone generator, simplified inductance networks can be drawn as in Figure 8.

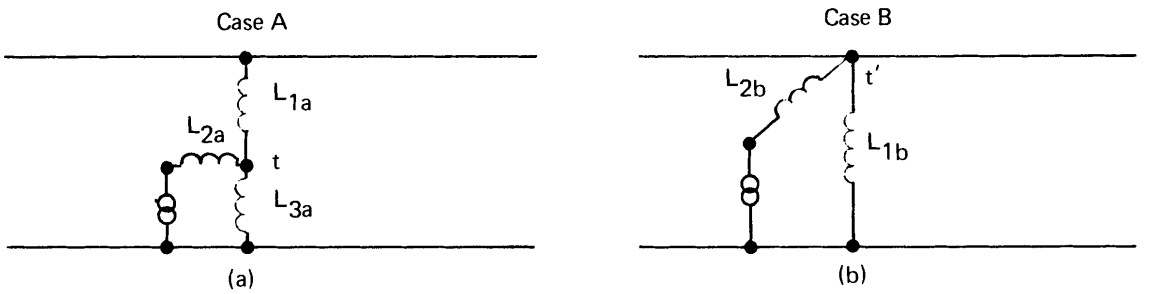

FIGURE 8 MODEL INDUCTANCE NETWORK

CASE A

In Case A the drop wire inductance formula (11) of Section C can be used for computing L_{1a},

$$L_{1a} = \frac{\mu D'}{2\pi} \ln\left(\frac{D}{r_o}\right) \qquad (12)$$

where $D' = D - 2a$, and r_o is the wire radius, in Figure 7a. The other inductance components of Cases A and B can be estimated using the following formula for a rectangular loop from Weber[3].

$$L = \frac{2\mu}{\pi}\left\{2\sqrt{a^2+b^2} + a \ln\left(\frac{8a}{d}\right) + b \ln\left(\frac{8b}{d}\right)\right.$$

$$-2(a+b) - a \ln\left[1+\sqrt{1+\left(\frac{b}{a}\right)^2}\right] \qquad (13)$$

$$\left.-b \ln\left[1+\sqrt{1+\left(\frac{a}{b}\right)^2}\right]\right\}$$

where 2a, 2b are the lengths of the rectangle sides and d is the wire diameter.

For Case A: $D = 5.5$ ft., $2a = 2b = 1$ ft., $d = 0.5$ in.

Therefore using (12) we get,

$$L_{1a} \simeq 1.5\mu\text{h}, \qquad (14)$$

and using (13), we get, $L \simeq 0.8\mu\text{h}$, (15)

for the square loop of Figure 7a. Now by separating out equal inductance contributions of 0.2μh for each leg of the square loop to form L_{2a} and L_{3a}, we get

$$L_{2a} \simeq 0.6\mu\text{h} \quad , \quad L_{3a} \simeq 0.2\mu\text{h}. \qquad (16a,b)$$

(3) E. Weber, "Electromagnetic Fields, Theory and Applications", Vol. 1, 1957, p. 131-133.

CASE B

For Case B: 2a = 5.5 ft., 2b = 1 ft., d = 0.5 in. Using Equation (13) for a rectangular loop we get:

$$L = 3.8\ \mu h. \qquad (17)$$

By approximating the inductance contribution of each short rectangular leg by the 0.2μh value for the square loop case, and therefore assigning 1.7μh to each long 5.5 ft. leg, we get:

$$L_{1b} = 1.7\mu h\ ,\ L_{2b} = 2.1\mu h. \qquad (18, 19)$$

Therefore, the simplified equivalent circuits become as shown in Figure 9 with the indicated impedance values at 88 kHz. These circuits are not meant to be exact representations, but simple approximations to provide workable means for estimating likely effects on performance. A more exact treatment would include the influence of mutual coupling on the specification of equivalent circuit components.

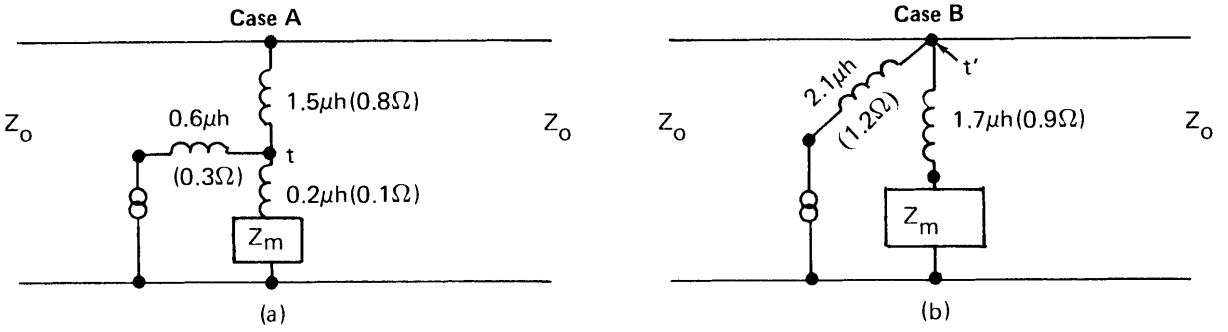

FIGURE 9 EQUIVALENT CIRCUITS

Raising the connection point, t, to the top of the trolley pole, t', changes the impedance level from [Z_m + 0.1 ohms (t-to-ground) to [Z_m + 0.9] ohms (t'-to-ground), an increase of only 0.8 ohms. In view of the high 200 ohm characteristic impedance of the trolley line, and the changing line impedance levels produced across the t'-to-ground connection as a result of other normal line loads, the small increase of about 0.8 ohms obtained by making connections at the top of the trolley pole appears to be grossly insufficient to provide significant improvements in trolley phone performance.

D. INDUCTANCE OF AIR-CORE COILS

Untuned air-core inductors have been and are still used in some mines to isolate the low impedance of rectifier power substations at the trolley phone frequency of 88 khz. This has been accomplished by forming a coil inductor consisting of about ten turns, three feet in diameter and three feet in length, which is placed in series with the substations. A good formula for estimating the approximate inductance of such air-core coils is given by

$$L = \frac{N^2\ r^2}{9r + 10\ell} \text{ in } \mu h \quad (4) \qquad (20)$$

where r is the coil radius in inches, ℓ is the coil length in inches, and N is the number of turns. For the above described coil, equation (20) predicts an inductance value of L = 62 μh, which results in an inductive reactance of 34 ohms at 88kHz. This value of reactance apparently is sufficient to improve trolley phone performance in many cases.

By resonating such an air-core coil with a parallel capacitance, much less inductance would be required to produce the desired impedance level. For example, using a circuit with a Q of 10, a desirable Q value for trolley phone applications, only 6.2μh are needed to get 34 ohms of reactance. Therefore a coil of the same number of turns and length would need only a diameter of 8.5 inches instead of 36 inches to produce the 6.2μh of inductance. If we further assume that the turns per unit length can be increased by at least a factor of two for the size wire required to carry the high current loads of coal mine trolley lines, then the length of the above 8.5 inch diameter coil can be reduced from 36 to 14 inches. Consequently, tuned air-core coils occupying about 1/2 cubic foot of volume may be practical alternatives, in some locations, to the ferrite or iron rf isolators described in Chapter III. The increased sensitivity of air-core coil behavior to nearby metal structures, however, may still make air-core coils less attractive for use in confined spaces as found inside locomotives.

E. THE EFFECT OF AN ATTACHED PARALLEL DC FEEDER CABLE ON TROLLEY LINE CHARACTERISTIC IMPEDANCE

At the Bethlehem Steel Marianna Mine in Uniontown, Pa., we noticed that the one million circular mil DC trolley feeder cable was made to run above, parallel to, and frequently connected to the trolley wire as shown in Figure 10.

---

(4) ITT Reference Data for Engineers, 5th Edition, Chapter 6, Fundamentals of Networks, pp. 6-3.

This kind of arrangement is sometimes used in mines to help maintain the

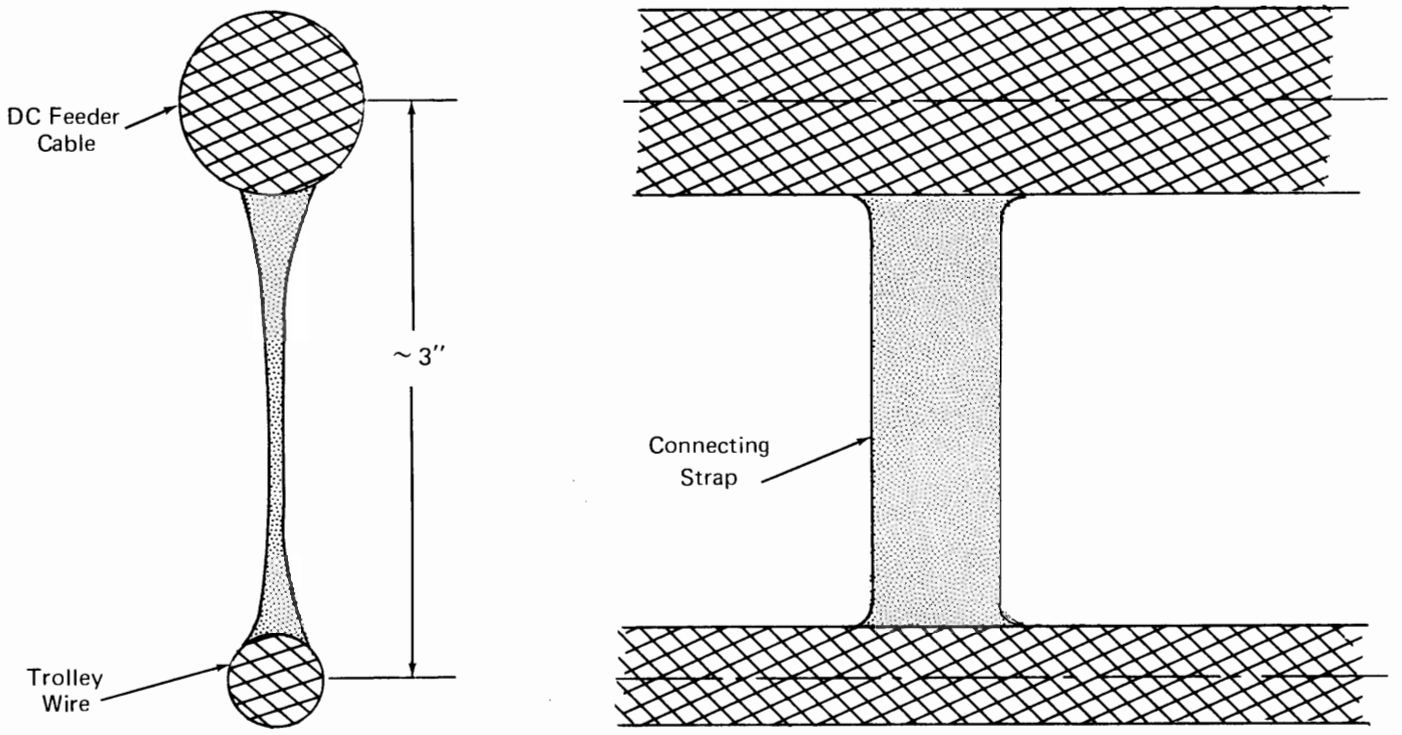

FIGURE 10 DC FEEDER CABLE AND TROLLEY WIRE GEOMETRIES

DC line voltage by decreasing the effective resistance of the trolley line, the diameter of which is only about 1/2 inch. Since this geometry increases the effective diameter of the trolley wire as far as the rf characteristic impedance of the line is concerned, an estimate was made of how much the characteristic impedance would be changed. An upper bound on this effect can be obtained by assuming that the Figure10geometry can be approximated by a cyclindrical wire of 3" diameter centered at the nominal 6" level down from the roof in a high-coal haulageway. Using equations 41a,b

$$Z_o = \frac{60}{\varepsilon^{1/2}} \cosh^{-1} U \qquad (21)$$

$$U = \frac{1}{2} [D/d + d/D - 4c^2/dD] \qquad (22)$$

$$c = D/2 - \delta \qquad (23)$$

with $\varepsilon = 1$, $d = 3''$, $D = 6'$, $\delta = 6''$,

$$\text{we get } \underline{Z_o = 118 \text{ ohms}}, \qquad (24)$$

which is about one-half the expected Z_o value for the trolley wire without the DC feeder cable.

The trolley wire at the Marianna mine was displaced, as is customary, about one foot to the outside of the rails as opposed to being centered above and between the rails as we first assumed. The utility of the eccentric line model of Figure (1) for such practical trolley line geometries should not be impaired, but in fact may even make the model more representative.

The lower Z_o value computed for the case of the DC feeder cable attachment also supports a measurement of net trolley line impedance as seen from our position near the shop area termination of the line. Figure 11 illustrates the track and trolley line routing in that immediate area. Trolley line continuity was maintained at the indicated branchings. Since all the distances to the branchings were small compared to wavelength at 88kHz, the network can be considered as five lines in parallel. If we further assume that each individual branch line looks matched in a characteristic impedance value of 118 ohms, then the net impedance seen at the starred shop location should be close to 24 ohms. A value of 22 ohms was measured with the PMSRC impedance measuring box. Future measurements should reveal whether this was just a coincidence.

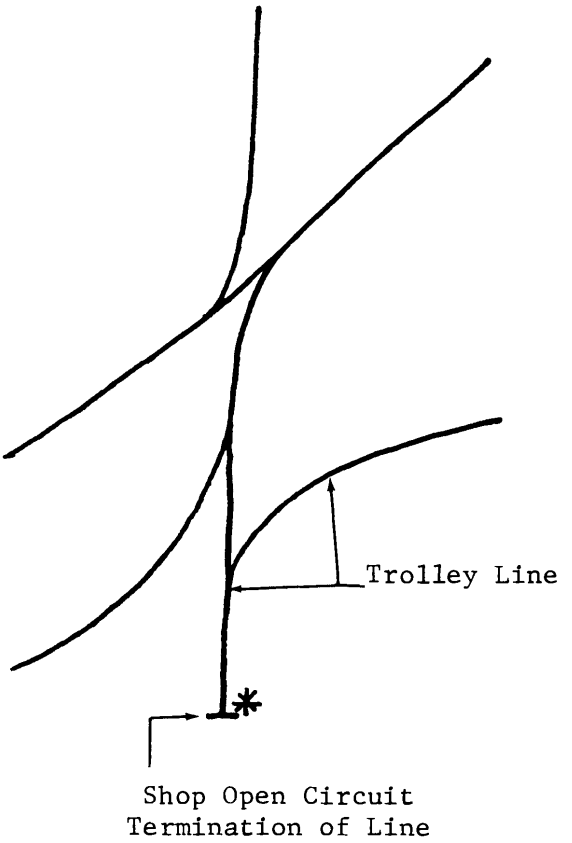

FIGURE 11 TROLLEY LINE ROUTING NEAR SHOP AREA

F. SOME TROLLEY LINE IMPEDANCE BEHAVIOR PREDICTED BY TRANSMISSION LINE THEORY

For a general lossy transmission line, the voltage and current along the line are given by

$$V(z) = V_+ e^{-\gamma z} + V_- e^{+\gamma z} \tag{25}$$

$$I(z) = \frac{1}{Z_o} [V_+ e^{-\gamma z} - V_- e^{+\gamma z}] \tag{26}$$

where $\gamma = \alpha + j\beta$ is the propagation constant and $Z_o = R + jX_o$ is the characteristic impedance.

Put in the classical convient form, we have

$$V(z) = V_+ e^{-\alpha z} e^{-j\beta z} [1 + \Gamma(z)] \tag{27}$$

$$I(z) = \frac{V_+ e^{-\alpha z} e^{-j\beta z}}{Z_o} [1 + \Gamma(z)] \tag{28}$$

where $\Gamma(z) = \frac{V_-}{V_+} e^{2\alpha z} e^{j2\beta z} = \Gamma_L e^{2\alpha z} e^{j2\beta z}$, is the reflection (29)

coefficient at an arbitrary point z on the line, and

$\Gamma(o) = \Gamma_L = \frac{V_-}{V_+}$ is the reflection coefficient of the load ter- (30)

minating the line at z = o. $\Gamma_{(o)} = \Gamma_L$ can be computed using

$\Gamma_L = \frac{Z_L - Z_o}{Z_L + Z_o}$, where Z_L is the impedance of the load. (31)

The geometry in question is shown in Figure 12.

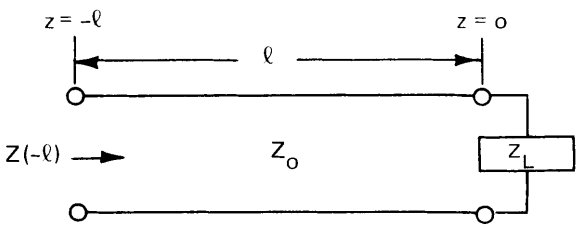

FIGURE 12 TRANSMISSION LINE AND LOAD IMPEDANCE

At a distance "ℓ" away from the load (e.g. $z = -\ell$), we get

$$V(z = -\ell) = V_+ \, e^{\alpha\ell} e^{j\beta\ell} [1 + \Gamma(-\ell)] \qquad (32)$$

$$I(z = -\ell) = \frac{V_+}{Z_o} \, e^{\alpha\ell} e^{j\beta\ell} \, [1 - \Gamma(-\ell)], \qquad (33)$$

so that the line impedance presented to a generator at $z = -\ell$ is given by

$$Z(-\ell) = \frac{V(-\ell)}{I(-\ell)} = Z_o \left[\frac{1 + \Gamma(-\ell)}{1 - \Gamma(-\ell)} \right]. \qquad (34)$$

$Z(-\ell)$ can be conveniently plotted in normalized form $Z(-\ell)/Z_o$ on a Smith Chart to examine its behavior as a function of line length, frequency, and the introduction of series and parallel loads.

The propagation constant and characteristic impedance are given by the following expressions.

Propagation Constant		Characteristic Impedance	
$\gamma = \sqrt{(R+j\omega L)\ (G+j\omega C)}$	(35)	$Z_o = \sqrt{\frac{R+j\omega L}{G+j\omega C}}$	(36)
$\gamma = \alpha + j\beta$	(37)	$Z_o = R_o + jX_o$	(38)

where R, G, L, C are the normal per unit length electrical parameters of the transmission line.

At first glance it appears that mine trolley lines can be considered "low loss" lines, having characteristic impedances that are essentially real, and lossless propagation constants $\gamma = j\beta = j\ 2\pi/\lambda$ modified by a small attenuation factor α, $\gamma = \alpha + j\beta$. Some investigators have observed attenuation rates on the order of 2 db per mile.* This is about 4 db per wavelength at 88 kHz, the wavelength being approximately 11,000 feet.

Using these values of wavelength and attenuation, the line impedance behavior produced by a short circuit placed across the line, as a function of distance away from the short circuit has been plotted on a Smith Chart in Figure 13. A short circuit was chosen as a first approximation to a DC rectifier power substation, and possibly a locomotive motor.

---

* More data are needed to determine whether this value is a representative one for different mines and installations.

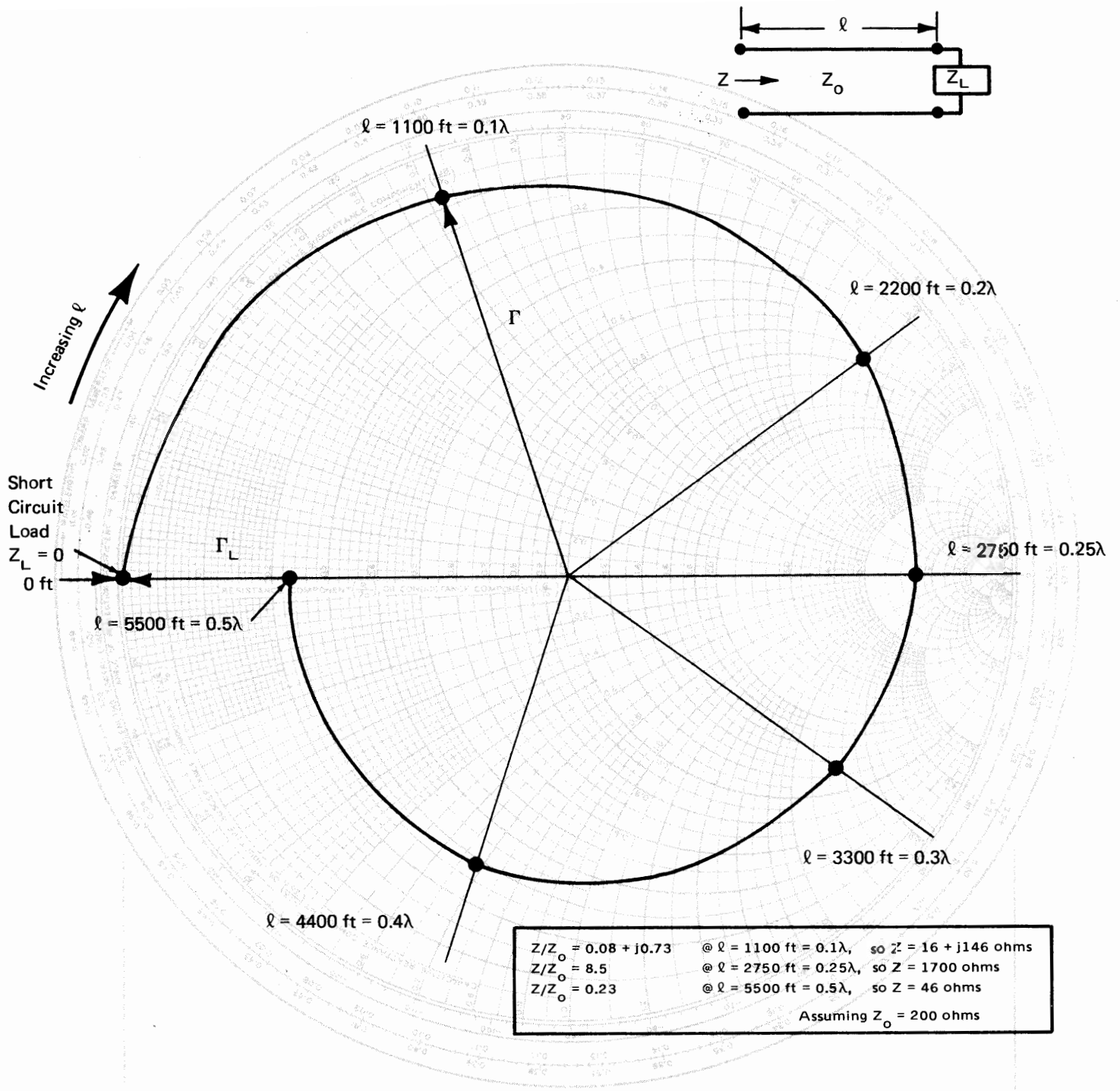

FIGURE 13 LOCUS OF NORMALIZED IMPEDANCE Z/Z_o ALONG LINE – CASE 1

For: Short Circuit Termination (Load)
Frequency – 88 kHz
Attenuation Factor: α = 4 dB per λ
(2 dB/mile)

The Smith Chart is used here as an impedance chart so that a short circuit of zero impedance occurs at the left hand side of the real (horizontal) axis. The reactance axis runs along the circumference, inductive reactance occurring in the top hemisphere and capacitive reactance in the lower. The real and imaginary impedance values are normalized to that of the characteristic impedance, Z_o. Distances expressed in fractions of a wavelength from the load moving towards the generator are also found along the circumference. Rotation once around the chart represents one-half wavelength of travel. The vector drawn from the center of the chart to any normalized impedance point is the reflection coefficient Γ. The center of the chart $Z/Z_o = 1 + j0$ describes the impedance $Z = Z_o$, namely that of a line matched to its characteristic impedance Z_o. Since power substations are spaced roughly a mile apart in typical coal mines, the impedance behavior has been plotted up to one mile away, which is roughly 1/2 wavelength at 88kHz. A short circuit $Z_L = 0$ represents a reflection coefficient $\Gamma_L = -1$. If the attenuation factor were zero, the Γ vector would be rotated at constant amplitude around the chart as the distance from the short increased, thereby giving rise to only reactive components of line impedance. Since the attenuation factor is not zero, but on the order of 4db per wavelength, the Γ vector will be reduced in size by twice this factor as prescribed by equation (29), thereby producing both resistive and reactive components of line impedance as the vector is rotated around the chart.

Examination of the Smith Chart plot of Figure 13 reveals several items of interest. It apparently is common practice in some mines to place the dispatcher's trolley phone station about 1000 feet from the DC substations in order to get satisfactory performance. From Figure 13 we see a healthy impedance level of $Z = 16 + j\ 146$ ohms is obtainable 1100 feet away from a substation short circuit placed across a $Z_o = 200$ ohm trolley line. Even if the Z_o is on the order of 100 ohms as may be the case in the Marianna mine, $Z \cong 8 + j\ 72$ ohms would be available. These reactive impedance values should be more than enough to allow satisfactory trolley phone signals to be put onto the trolley line from a 25 ohm transmitter, if the transmitter is not adversely affected by reactive loads, thereby supporting the above practice. Figure 13 also indicates that a mobile unit should encounter its worst performance, due to the presence of a low impedance substation or mine motor, when the mobile is in the immediate vicinity of the substation or motor, say within about 100 feet. Once beyond the very low impedance region near the substation or motor, the magnitude of the impedance will not decrease below the 46 ohm level found at the one-half wavelength distance, for the line described. The finite attenuation factor makes the impedance locus gradually spiral in towards the center of the Smith Chart. This prevents the impedance from going to zero again at the half wave length distances, and eventually makes Z approach the Z_o value if no other impedances are placed across the line. The finite attenuation factor also prevents infinite values of impedance from occurring at the quarter wavelength distances, a maximum of 1700 ohms being the upper limit at $\lambda/4$ for the case described.

One last case of interest is that of a 25 ohm resistive trolley phone load. The impedance variation as a function of line length for the 25 ohm resistive load has been plotted in Figure 14. Note that reactive impedances are still produced, but that the maximum impedance level achieved (at $\lambda/4$) is half of that for the short circuit case, while the $\lambda/2$ impedance value has been increased by half again over that for the short circuit case, for the line in question. The effects of placing additional 25 ohm and/or short circuit "mobile" loads across the line at arbitrary locations can also be treated. This can most conveniently be done by using the Smith Chart as an admittance chart, which allows the addition of parallel admitances in a simple manner graphically. However, one can get a good feel for the impedance behavior expected at an arbitrary attachment point between two loads on a continuous line by placing to the left of the $z = -\ell$ point of Figure 12, a second line section of length ℓ' and load Z_L' appropriate to what is present to the left of the attachment point; computing the impedance seen looking to the left Z_ℓ per Figures 13 and 14; and summing them together as a parallel impedance connection.

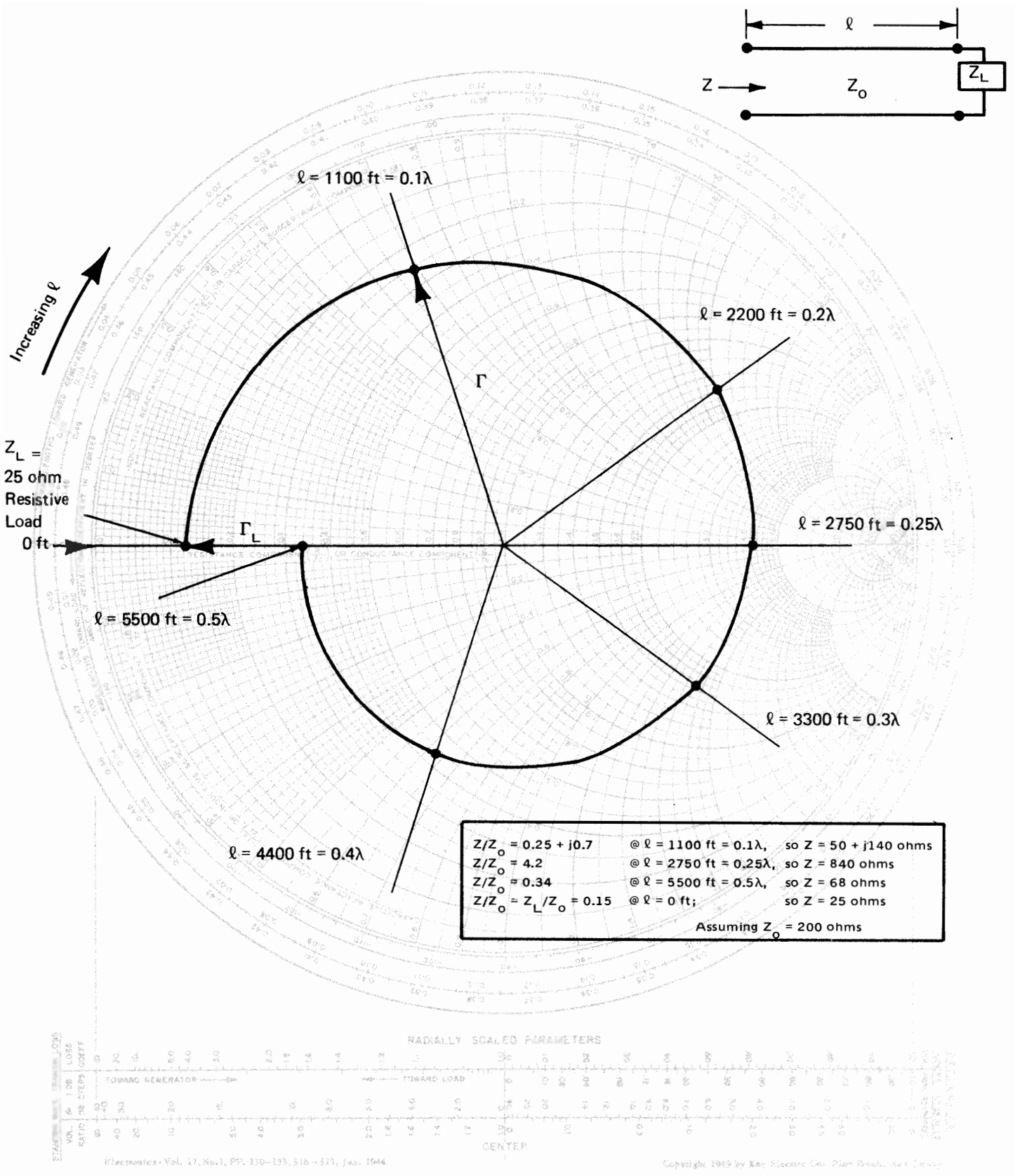

FIGURE 14 LOCUS OF NORMALIZED IMPEDANCE Z/Z_o ALONG LINE – CASE 2

For: 25 ohm Resistive Termination (Load)
Frequency – 88 kHz
Attenuation Factor: α = 4 dB per λ
(2 dB/mile)

G. CHARACTERISTIC IMPEDANCE ESTIMATES FOR MINE TROLLEY LINES

The characteristic impedance of a uniform transmission line is given by

$$Z_o = \sqrt{\frac{R+j\omega L}{G+j\omega C}} \text{ ohms} \qquad (39)$$

where ω is the radian frequency, R and L are the series resistance and inductance per unit length, and G and C are the shunt conductance and capacitance per unit length. For lossless lines, which most practical lines approach, R and G = 0. Then Z_o reduces to

$$Z_o = \sqrt{\frac{L}{C}} \ , \qquad (40)$$

and the characteristic impedance is a function only of the cross-sectional geometry and the dielectric and magnetic properties of the cross-sectional media.

To get a first-order analytical estimate of Z_o for trolley lines in coal mines, losses were neglected and the mine haulageway geometry approximated by some classical geometries for which equations are readily available for Z_o. The trolley haulageway cross-sections in Figure 15 are considered representative.

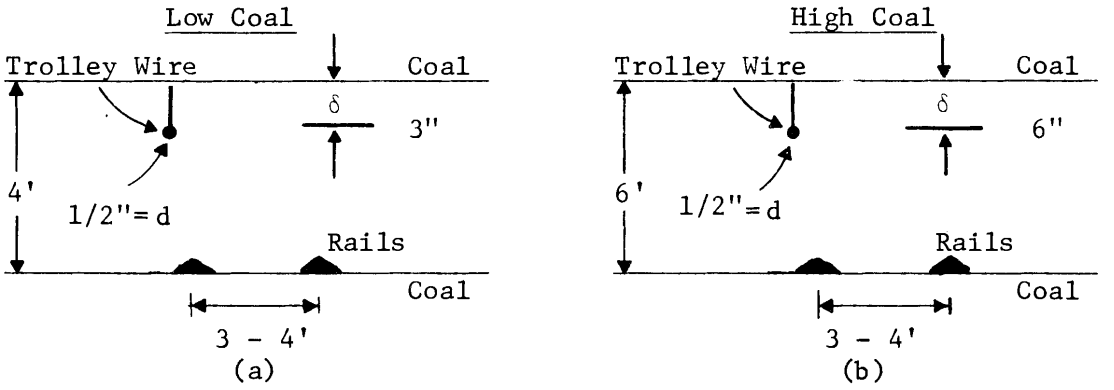

FIGURE 15 CROSS-SECTIONAL VIEWS OF TROLLEY LINE GEOMETRIES

The trolley transmission line consists of an overhead trolley wire isolated from the haulageway ceiling, together with two trolley rails serving as return path conductors. The rails are in turn grounded to the coal which has a moderate conductivity ranging from about 10^{-1} to 10^{-3} mho/meter. So the surrounding coal may produce behavior similar to that of a ground plane in place of the rails, or that of a surrounding conducting shield.

1. Impedances for Approximate Geometries

Two geometries, with readily available equations for Z_o, that may approximate these trolley wire situations, are shown in Figures 16 and 17. Figure 16 is Case 1, an eccentric shielded line, and Figure 17 is Case 2, a single wire above a ground plane. Two other cases that do not include the effects of the surrounding coal are also included for ready comparison. They are Case 3, the open two-wire line with unequal diameters in Figure 18 and Case 4, open two-wire line with equal diameters in Figure 19.

Case 1: Eccentric Line

$$Z_o = \frac{60}{\varepsilon^{1/2}} \cosh^{-1} U \qquad (41a,b)$$

$$U = \tfrac{1}{2} [D/d + d/D - 4C^2/dD]$$

$\varepsilon = 1$, $d = 0.46"$, $C = \frac{D}{2} - \delta$

D(variable) 3 to 10 ft., δ = 3" low coal, 6" high coal

Case 2: Single Wire Above a Ground Plane

$$Z_o = \frac{138}{\varepsilon^{1/2}} \log_{10} (4D/d) \text{ for } d \ll h \qquad (42)$$

$\varepsilon = 1$, d = 0.46" nominal diameter of 0000 trolley wire

D(variable) 3 to 10 ft. - (low to high coal)

Case 3: Open Two-Wire Line with Unequal Diameters

$$Z_o = \frac{60}{\varepsilon^{1/2}} \cosh^{-1} N \qquad (43a,b)$$

$$N = \tfrac{1}{2} \left[\frac{4D^2}{d_1 d_2} - \frac{d_1}{d_2} - \frac{d_2}{d_1} \right]$$

$\varepsilon = 1$, $d_2 = 0.46"$, D(variable) - 3 to 10 ft.

Do for two values of d_1

$d_1' = 4.6"$ approximate diameter of a single rail

$d_1'' = 46"$ approximate maximum separation between rails--assuming a cylinder of that diameter

Eccentric Line

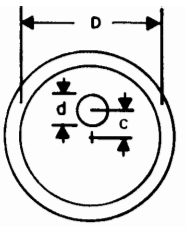

$$Z_0 = (60/\epsilon^{1/2}) \cosh^{-1} U$$

$$U = \tfrac{1}{2}\left[(D/d) + (d/D) - (4c^2/dD)\right]$$

FIGURE 16 CASE 1

Single wire, near ground

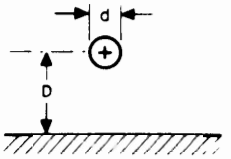

For $d \ll D$

$$Z_0 = (138/\epsilon^{1/2}) \log_{10}(4D/d)$$

FIGURE 17 CASE 2

Balanced 2-wire—unequal diameters

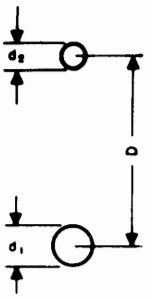

$$Z_0 = (60/\epsilon^{1/2}) \cosh^{-1} N$$

$$N = \tfrac{1}{2}\left[(4D^2/d_1 d_2) - (d_1/d_2) - (d_2/d_1)\right]$$

FIGURE 18 CASE 3

Open 2-wire line in air

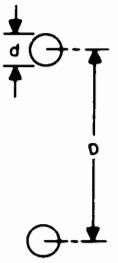

$$Z_0 = 120 \cosh^{-1}(D/d)$$
$$\approx 276 \log_{10}(2D/d)$$
$$\approx 120 \log_e(2D/d)$$

FIGURE 19 CASE 4

Source: *ITT Reference Data for Radio Engineers,* 5th Edition Chapter 22

Case 4: Open Two-Wire Line

$$Z_o = 120 \cosh^{-1} (D/d) \qquad (44)$$

d = 0.46", D(variable) - 3 to 10 feet.

The computed values of characteristic impedance for each case are presented in Figure 20 for convenient comparison of limits, trends, and effects of nearby conducting walls or floors.

2. Discussion of Results

Examination of Figure 20 and the equations reveals that once the spacing D becomes large compared to the trolley wire diameter d, the characteristic impedance is not very sensitive to further increases in D. Furthermore, the oversimplified geometries of Cases 3 and 4 give values of Z_o that far exceed any line impedance values apparently encountered to date in mines. Case 2, although giving lower values, still appears somewhat high. Only Cases 1a and 1b approach the high side of the impedance values that have been observed experimentally by past investigators on trolley lines under typical conditions. Z_o for the Case 1 structure is relatively insensitive to both the roof-to-floor distance D and the distance d of the trolley wire from the roof, for values typical of those found in mines. Similarly, other investigators have experimentally observed only small changes in trolley line Z_o behavior under both high and low coal conditions.

The above calculations indicate that the Z_o's of lossless lines with geometries and dimensions similar to coal mine trolley lines will not fall much below about 200 ohms. The presence of substantial distributed shunt loss, G, with its corresponding high attenuation, could reduce Z_o dramatically from its lossless line value. However, other investigators have observed only little attenuation (approximately 2db per mile) on long runs of trolley line. Consequently, the variable impedance values (generally below 200 ohms) often observed on trolley lines, are most likely caused by the moving low impedance motor loads placed across the trolley lines via locomotive trolley poles. Therefore, in our quest for a solution to motor loading, the Case 1 eccentric line structure with a nominal Z_o value of Z_o = 200 ohms, presently looks like a reasonable approximation to use for haulageway trolley lines.

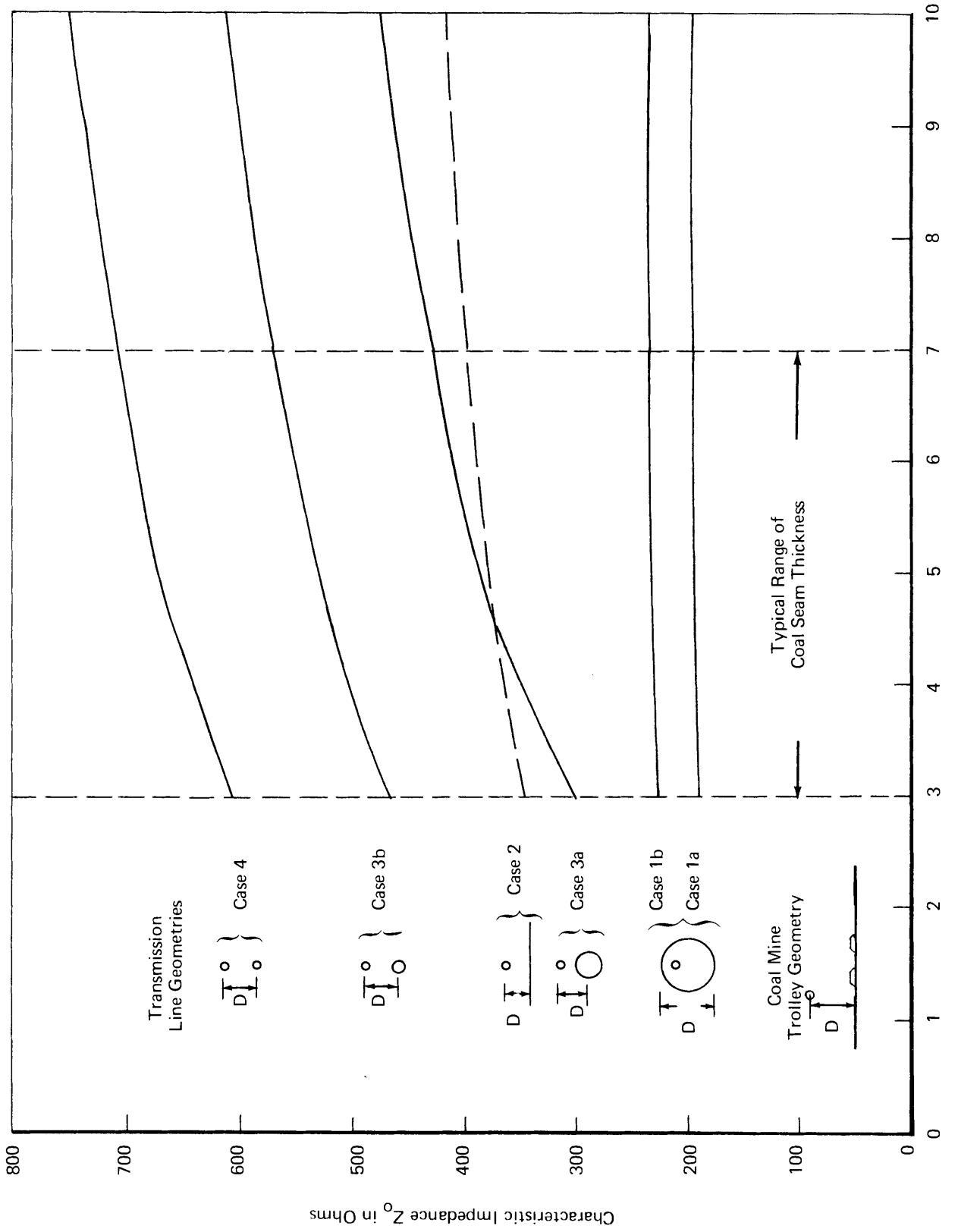

FIGURE 20 PLOTS OF CHARACTERISTIC IMPEDANCE Z_o VERSUS D

II. RF ISOLATORS FOR MINE MOTORS

A. BACKGROUND

The mine trolley phone systems presently in use can frequently suffer from low signal strength problems attributed to trolley motors acting as extremely low impedances across the trolley line signal pair used for the transmission of carrier communication signals. To obviate the problem caused by these low impedance "shorts", it is desirable to add impedance in series with the trolley motors, thus preventing each trolley motor from acting as a signal "short".

The most severe problem met in implementing such a scheme is due to the fact that, while providing the added impedance at the carrier frequency (typically 88 kHz or 100 kHz), it must: act as an extremely low resistance at dc, be able to pass up 2000 amperes without sustaining damage, and be able to maintain its 88 kHz impedance level while passing in excess of 400 dc amperes.*

B. APPROACH

Techniques that have been used in power and electronic systems suggest a means of adding the desired impedance to a trolley without imposing difficulties in installation or any added dc resistance. One of these techniques is the use of a single-turn transformer winding, such as the current transformers with single-turn primaries commonly used in power monitoring systems. A second technique is one commonly used in digital electronic printed circuit boards. Most of the circuits found on these boards are extremely sensitive to electrical spikes that occur on power supply lines. Frequently, use is made of a ferrite toroid together with a capacitor. The power supply lead is fed through the toroid, thus adding inductance to the power supply line. This inductance, combined with the capacitor, serves to block the voltage spikes from penetrating to the sensitive circuit elements.

---

*We have since learned that a 400 ampere operating current is more typical of small 10-12 ton locomotives on 600V DC trolley lines, and not of the more important 50-ton locomotives on 300V dc lines which will draw 3000-4000 amperes under full load conditions. Under these 3000-4000 amperes current conditions, the isolators designed for 400 ampere dc currents will saturate and be totally ineffective. If provisions are made to prevent saturation until beyond 4000 amperes by increasing the core air gap, the isolators in their present configuration will have to be increased beyond their present overall length of 6 inches by about a factor of 10 to maintain the required inductance to produce the desired 20 ohm isolator impedance at 88kHz. The cost, length, and weight of such a 4000 ampere unit is no longer as attractive as the 400 ampere unit, and as such is probably an impractical isolator solution for 50-ton locomotives. Special ferrite castings to improve the core geometry, and therefore, reduce the overall volume of the core may be possible, but significant reductions in volume don't look too promising upon first examination.

A representation of how such a technique can be applied to the trolley problem is illustrated in Figure 1A.* Figure 1B* shows an equivalent circuit for the configuration of Figure 1A. In this equivalent circuit, the terminal-to-terminal impedance is that which is added in series with the trolley. It should be noted that the magnetic element does not affect the trolley cable in terms of dc resistance, since the capacitor and resistor are inductively coupled to the core as opposed to being connected to the trolley wire. The equivalent circuit shows that there can be considerable impedance at the carrier frequency if the circuit is tuned to the carrier. The capacitor is used to accomplish this tuning, while the resistor is used to set the Q or quality factor of the circuit, and thus the circuit impedance ($Z = Q\omega_o L$) at the carrier frequency.

There are two problems associated with implemeting this scheme. First, and most important, the magnetic core is subject to saturation by the very substantial dc currents drawn by the trolley motors. Secondly, the transformer must have sufficient Q at the carrier frequency in order that tuning will produce the desired impedance value.

We have investigated several materials which seemed to be potentially applicable for this use, and the following conclusions apply:

1. Powdered iron cores. In principle these cores will perform the function; however, the cost is high.

2. Laminated transformer iron. The effective μ and quality factor at 88kHz are marginal, while the cost and weight are also high.

3. Ferrite materials. The cost is moderate, the μ and quality factors are adequate, but the saturation levels marginal for trolley applications.

The following target specifications were set by us for an rf isolator of this type:

- DC current rating: 0 to 2000 amperes (without damage to circuit).

- DC operating current: 0 to 400 amperes (impedance will be within $\pm$ 30% of target).

- Impedance: Larger than 20 ohms at 88kHz or at 100kHz.

- Bandwidth: 8.8kHz or 10kHz.

---

* References to Figures, Tables, and Equations apply to those in this Chapter unless otherwise noted.

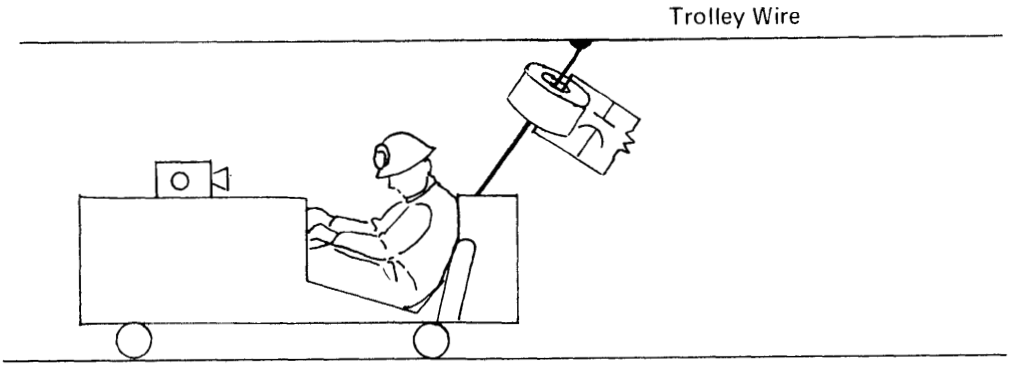

FIGURE 1A REPRESENTATION OF SINGLE-TURN COUPLED IMPEDANCE ELEMENT INSTALLED ON A TROLLEY POLE

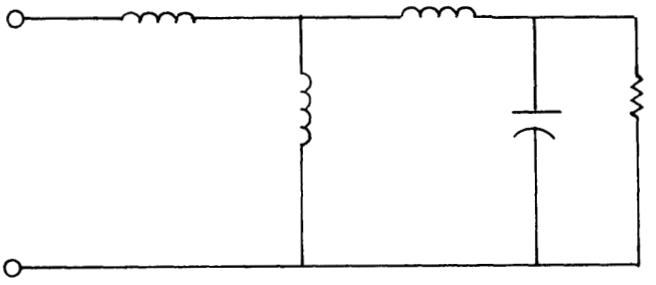

FIGURE 1B EQUIVALENT CIRCUIT OF IMPEDANCE ELEMENT

C. DESIGN CALCULATIONS

The first-order design is extremely simple and for most configurations yields results within several percent of actual design values. Consider the core configuration as shown in Figure 2. The reluctance of the magnetic path is:

$$R = \frac{1}{A}\left(\frac{\ell_M}{\mu_M} + \frac{\ell_A}{\mu_A}\right) \qquad (1)^*$$

where ℓ_M = length of path in magnetic material

ℓ_A = length of path in air

μ_M = permeability of magnetic material

μ_A = permeability of air.

If the μ of the magnetic material is 1000 times that of air, then for an air gap that is more than 1/100 of the magnetic path length, the reluctance and hence the inductance of a winding on the core is dominated by the air gap. Thus, for our purposes where the air gap and magnetic material paths are known to have about the right relationships, the first-order design proceeds on the basis that the air gap dominates completely. This fact is true up to the point where the dc current, and hence the magnetic flux density, becomes so large that the magnetic material saturates and reduces the effective permeability to a value significantly less than 1000.

The design procedure is to select the value of flux density (B_o gauss) in the magnetic material at which the incremental permeability is reduced by saturation to the minimum acceptable value. The air gap in the magnetic path is selected so that the maximum motor current for which the isolator must work, I_o, produces just this flux density in the gap and in the magnetic material. Because we are dealing with a single turn, the number of ampere turns becomes I_o, the flux density is B_o, and the magnetic field intensity H in the air gap numerically equals B_o expressed in oersteds (cgs units). The ampere turns per inch then become

$$\frac{I_o}{\ell_A} = H = B_o. \qquad (2)$$

Thus the air gap is given by

$$\ell_A = \frac{I_o}{B_o}\ \text{cm} = \frac{I_o}{B_o(2.54)}\ \text{inch}. \qquad (3)$$

---

* References to Figures, Tables, and Equations apply to those in this Chapter unless otherwise noted.

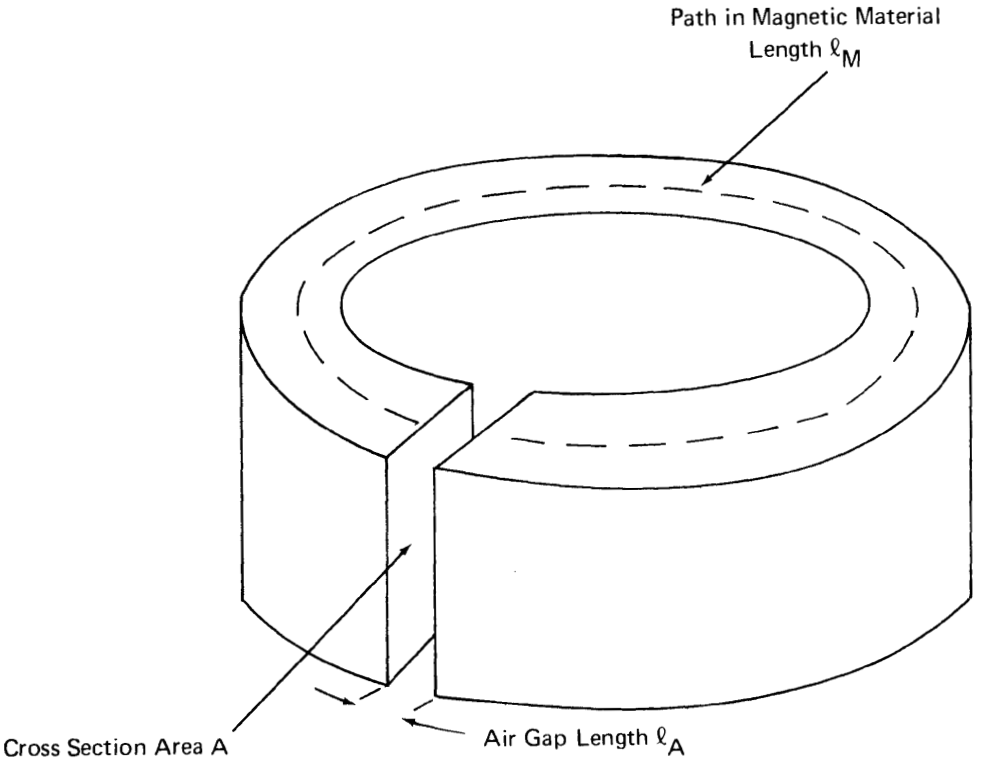

FIGURE 2 TOROID WITH AIR GAP

The inductance is $L = \frac{\lambda}{I_o} = \frac{B_o A}{I_o}$ (4)

where λ equals flux linkages in Weber turns, I_o in amperes, and A is cross-sectional area.

Thus we can plot the inductance per unit area as a function of I_o for various candidate materials. The Ferroxcube, 3C5 material, can be operated at 2500 gauss and still maintain sufficient incremental permeability for the air gap to dominate. A plot of inductance per square inch of cross-section for this material is shown in Figure 3. Using this plot one can determine the core cross-section area required to meet a specific design. As an example, assume that the isolator must function for currents up to 400 amperes. From the plot of Figure 3, it is seen that an inductance of .4 microhenries per square inch is usable.*

The desired resonant impedance is 20 ohms. For a Q of 10, this impedance is ten times the inductive reactance provided by the core itself at 88kHz. Thus the inductive reactance required of the core is 2 ohms, corresponding to an inductance of 3.68 microhenries. The cross-sectional area required is thus 9.2 square inches. Were arbitrary shapes of ferrite material available, one could select the shape that would provide this cross-sectional area to best match the space available in a locomotive for installation. For example, a toroid of outside diameter 5", inside diameter 1", and a length of 4.5" would provide the required core cross-sectional area. Similar calculations can be performed for both larger and smaller current ratings.

D. LABORATORY TEST DATA

Unfortunately, for present experimental investigations, use must be made of available cores which are quite limited in the sizes and shape factors that are attractive for our purpose. We have done experiments on available standard cores. The results of these experiments are shown in Figure 4, which illustrates the effects of the saturation of a ferrite core pair.

These data were sufficiently encouraging that a set of tuned isolators were assembled for test in a laboratory in preparation for field evaluation in an actual trolley phone system. The goal was to achieve a 20 ohms impedance at 88kHz with a bandwidth of 8.8kHz and a dc operating current rating of 400 amperes. We believe that a rating of 400 amperes will suffice for many conditions**, although it does preclude operation during starting and under extremely

*Similar calculations were made for powdered iron and laminated iron cores. The powdered iron cores were rejected on the basis of excessive cost. Laminated cores with 4 mil and 2 mil thick laminations were purchased and tested as were the ferrite cores. The laminated cores were then rejected because their inadequate Q factor required an excessive number of the expensive cores to achieve the desired impedance.

** See note on first page of this Chapter.

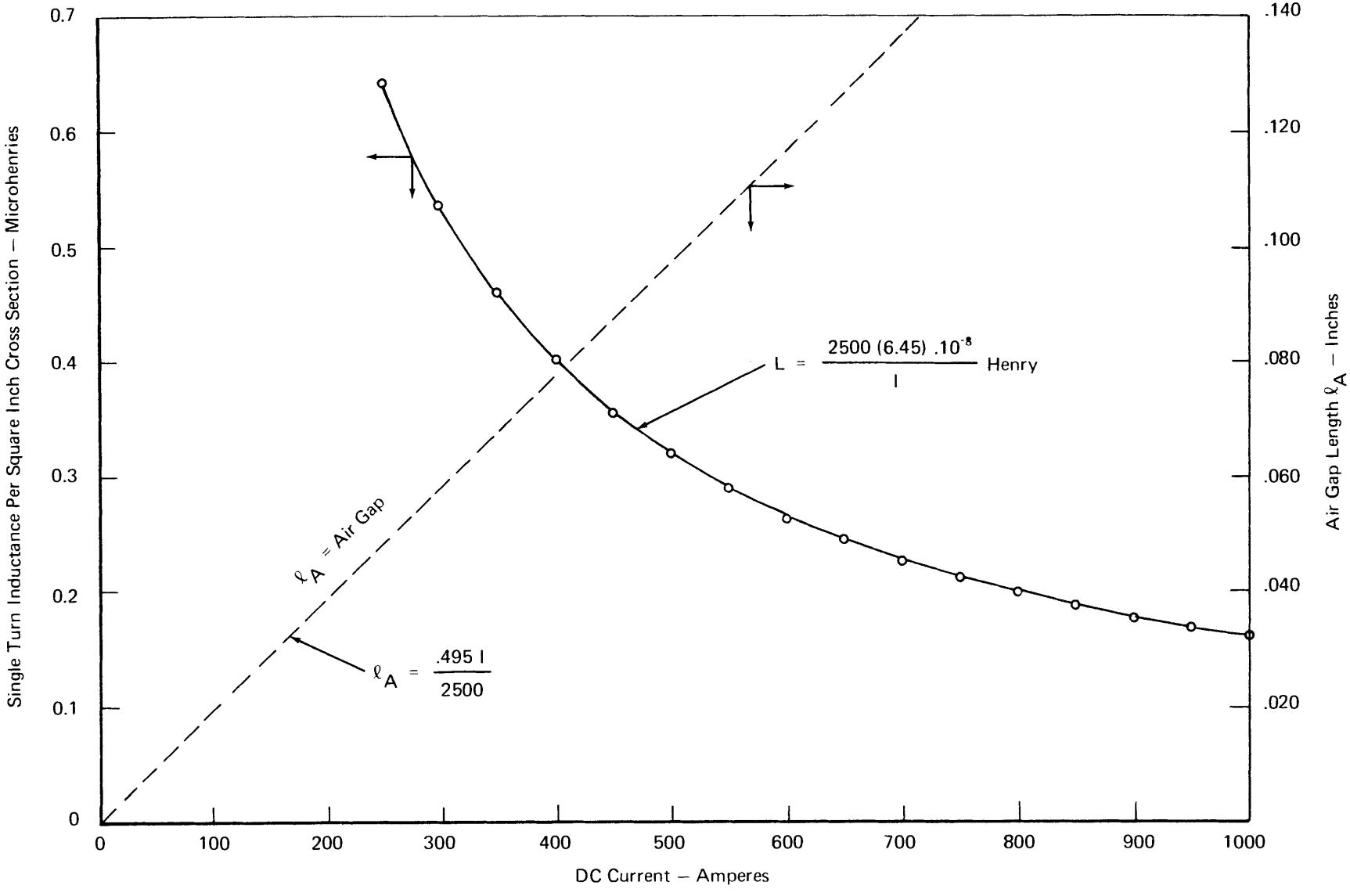

FIGURE 3 FERROXCUBE 3C5 MATERIAL INDUCTANCE PER SQUARE INCH OF CROSS SECTION VERSUS MAXIMUM DC CURRENT – SINGLE TURN WINDING

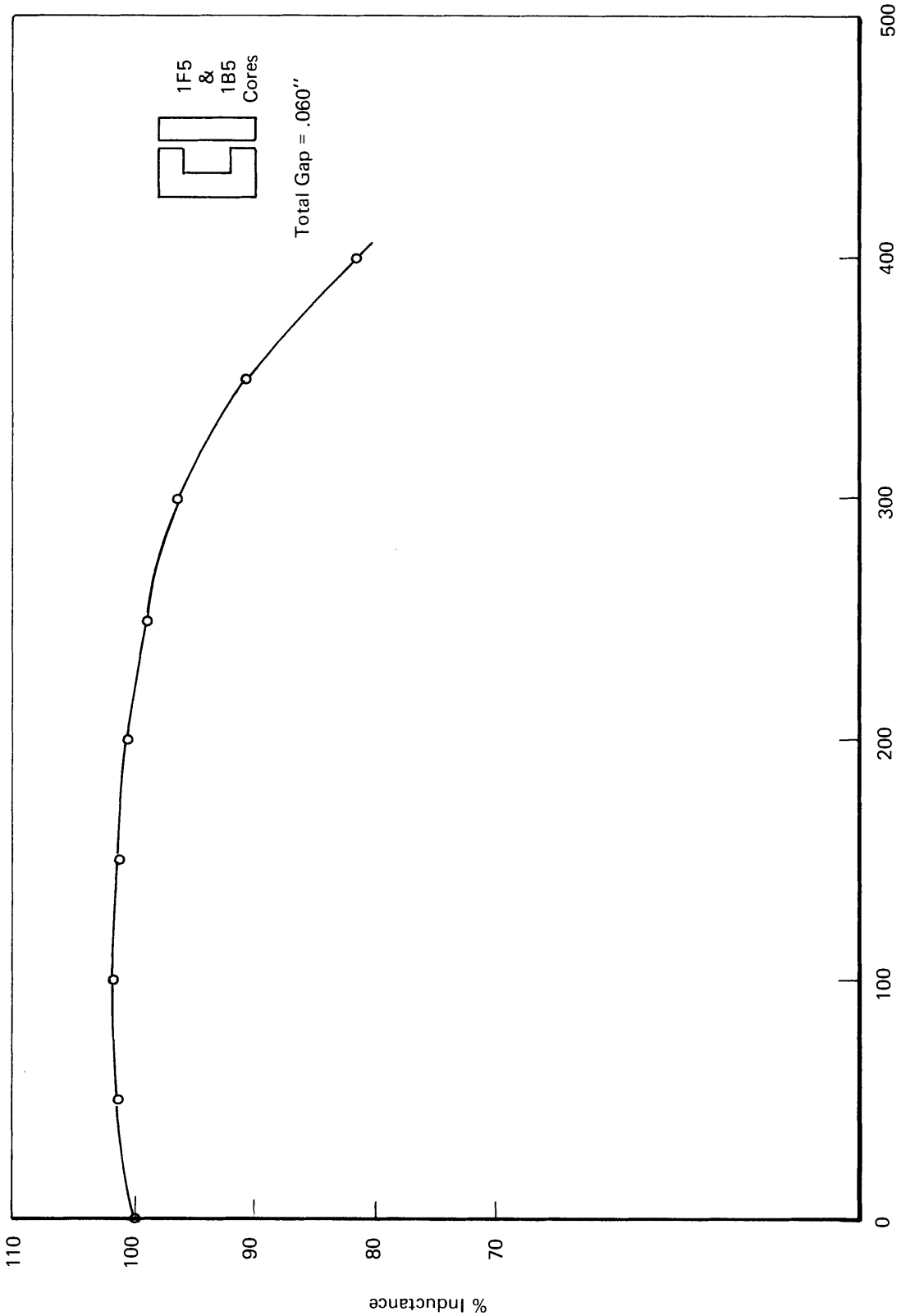

FIGURE 4 INDUCTANCE VERSUS CURRENT

heavy load conditions. The system will not be damaged by much larger currents but will merely be detuned from 88kHz. The isolater unit was comprised of six U sections and six I sections of a standard commercial ferrite core as shown in Figure 5. The configuration of the isolator is illustrated in Figure 6. For this configuration the reluctance:

$$R = \frac{1}{A}\left(\frac{\ell_M}{\mu_M} + \frac{\ell_A}{\mu_A}\right) \quad \text{and} \tag{5}$$

$$L = \frac{A}{\left(\frac{\mu_A}{\mu_M} + \ell_A\right)} \tag{6}$$

and thus the inductance $L = \dfrac{(6.45) \times 10^{-8}}{2.54\ (\frac{10.5}{1500} + \ell_A)}$ henry. (7)

The magnetic material path length ℓ_M is 10.5 inches, μ_M is assumed to be 1500, and A is 1 square inch.

A plot of the calculated and measured inductance for a single pair of these cores is shown in Figure 7. The Q when tuned to 88kHz was between 20-30. The measured value of inductance is higher than the calculated for most points. This can be attributed to the fact that the relatively large air gaps cause part of the flux to follow paths outside the air gap. These uncertainties mean that while the formulas discussed above are useful in determining the nominal values of circuit parameters, their exact values will have to be determined emperically. An optional resistor may be added in parallel with the tuning capacitor to adjust the Q downward if desired.

E. CONCLUDING REMARKS

An isolator made of Ferroxcube 3C5 ferrite that provides 20 ohms impedance at 88kHz in the face of 400 amperes dc current, with a bandwidth of 8.8kHz, weighs 8.7 lbs., and has outside dimensions of 4-1/2" x 4-1/4" x 6" when made of available core parts. This isolator has an opening of 1.25" x 2" as a passage for the power cable. Cost of the core parts in small quantities is $48.

We recommend that experiments be done on a trolley phone system to test isolator performance under typical conditions. A minimum experiment would involve measuring the trolley line rf voltage as a locomotive passes a measuring station for different levels of locomotive power, both with and without the rf isolator described above.*

*A very short experiment similar to this was performed at the Bethlehem Steel Marianna Mine in Ellsworth, Pennsylvania on a 50 ton tandem locomotive. Rf line voltage was measured under stationary simulated load conditions of applying full power to 1, 2 or 4 motors with full braking also applied. Full rf voltage appeared as expected under no-load conditions, but dropped essentially to levels achieved in the absence of the isolator under all three load conditions, becasue the 400 ampere saturation rating was exceeded for all 3 loads. Further detailed inquiry of mine operators and equipment manufacturers revealed the 3000-4000 ampere loads typical of 50-ton locomotives operating at 275 volts, and led to the conclusions of the asterisked note on the first page of this Chapter.

5 U CORE 1F5

U CORE, Part Number 1F5
I CORE, Part Number 1B5

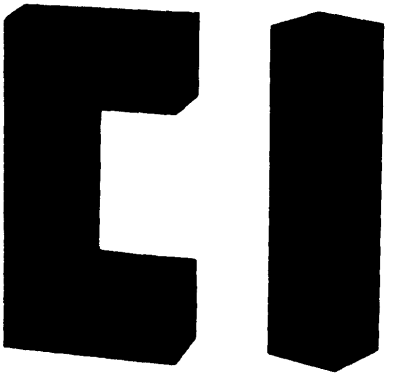

HALF ACTUAL SIZE

This core is

- manufactured in 3C5 ferrite material only.
  (See Section 1 for material characteristics)
- available in U-U and U-I configurations.
  (for a complete U-I core set, specify both part numbers)
- not available with bobbins or mounting hardware.

When ordering cores, specify core part number and ferrite material.
e.g.: 1F5–3C5 or 1B5–3C5

CHARACTERISTICS & DIMENSIONS

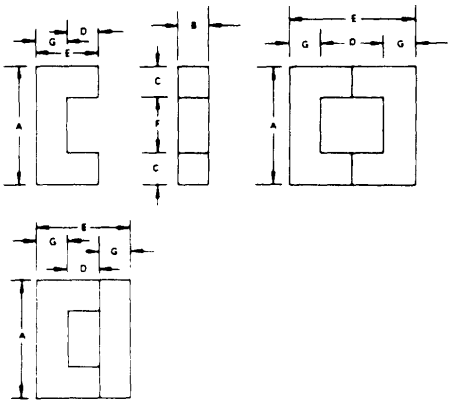

NOMINAL DIMENSIONS IN INCHES

DIMENSION	SINGLE U CORE	U-U	U-I
A	4.00	4.00	4.00
B	1.00	1.00	1.00
C	1.00	1.00	1.00
D	1.25	2.50	1.25
E	2.25	4.50	3.250
F	2.00	2.00	2.00
G	1.00	1.00	1.00

ELECTRICAL CHARACTERISTICS

CONFIGURATION	U-U	U-I	U-U	U-I
A_L mH per 1000 turns	⩾5500	⩾6900	⩾7850	⩾9850
μ_e ref. (min.)	2100 at 25°C 1000 Gauss		3000 at 100°C 2000 Gauss	

MECHANICAL CHARACTERISTICS

CORE SET		U-U	U-I
MAGNETIC PATH LENGTH	ℓ_e	12.4 in. 31.5 CM	9.64 in. 24.5 CM
CORE CONSTANT	$\Sigma \frac{\ell_e}{A_e}$	12.4 $in.^{-1}$ 4.884 CM^{-1}	9.64 $in.^{-1}$ 3.798 CM^{-1}
EFFECTIVE CORE AREA	A_e	1.00 $in.^2$ 6.45 CM^2	1.00 $in.^2$ 6.45 CM^2
EFFECTIVE CORE VOLUME	V_e	12.1 $in.^3$ 198 CM^3	9.64 $in.^3$ 158 CM^3
WINDING AREA	A_c	5.00 $in.^2$ 32.25 CM^2	2.50 $in.^2$ 16.125 CM^2
WEIGHT		32.5 oz. 930 grams	23.1 oz. 660 grams

5-12

Source: Ferroxcube Corp., *Linear Ferrite Materials & Components Catalogue*

FIGURE 5 CORES USED IN EXPERIMENT

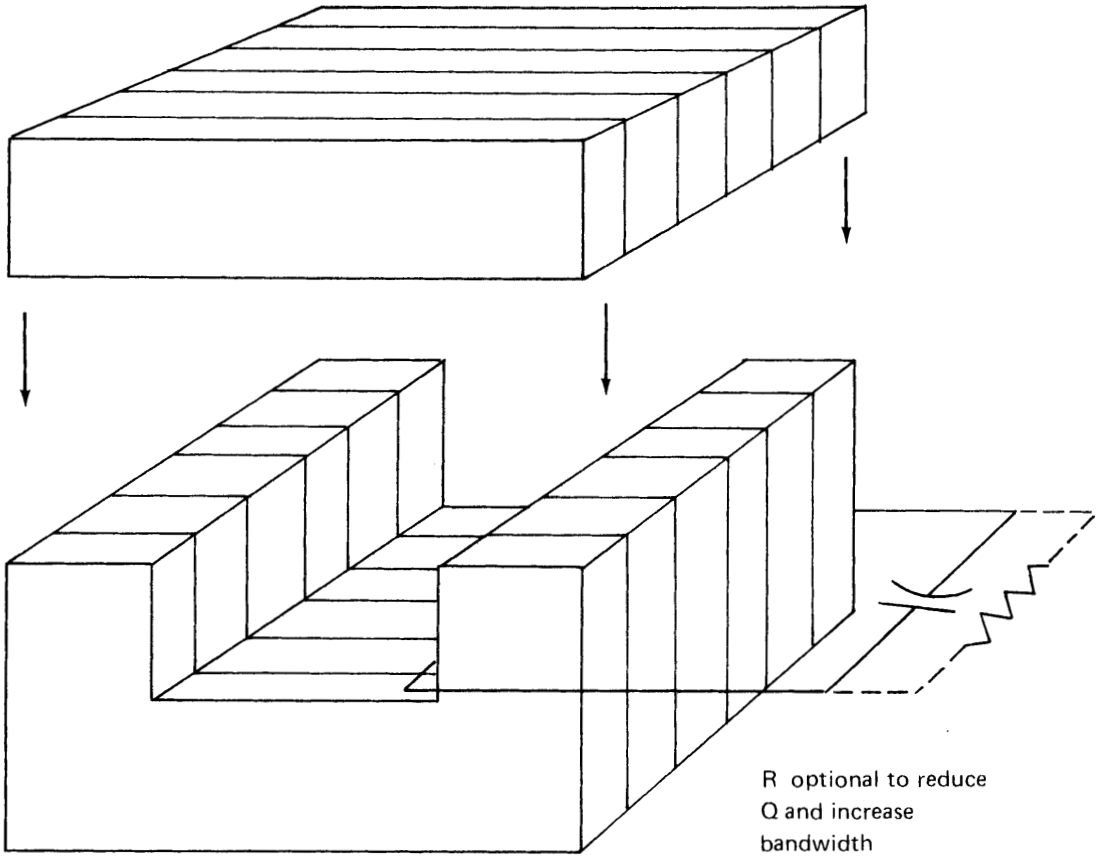

FIGURE 6 CONFIGURATION OF CORES FOR ISOLATOR

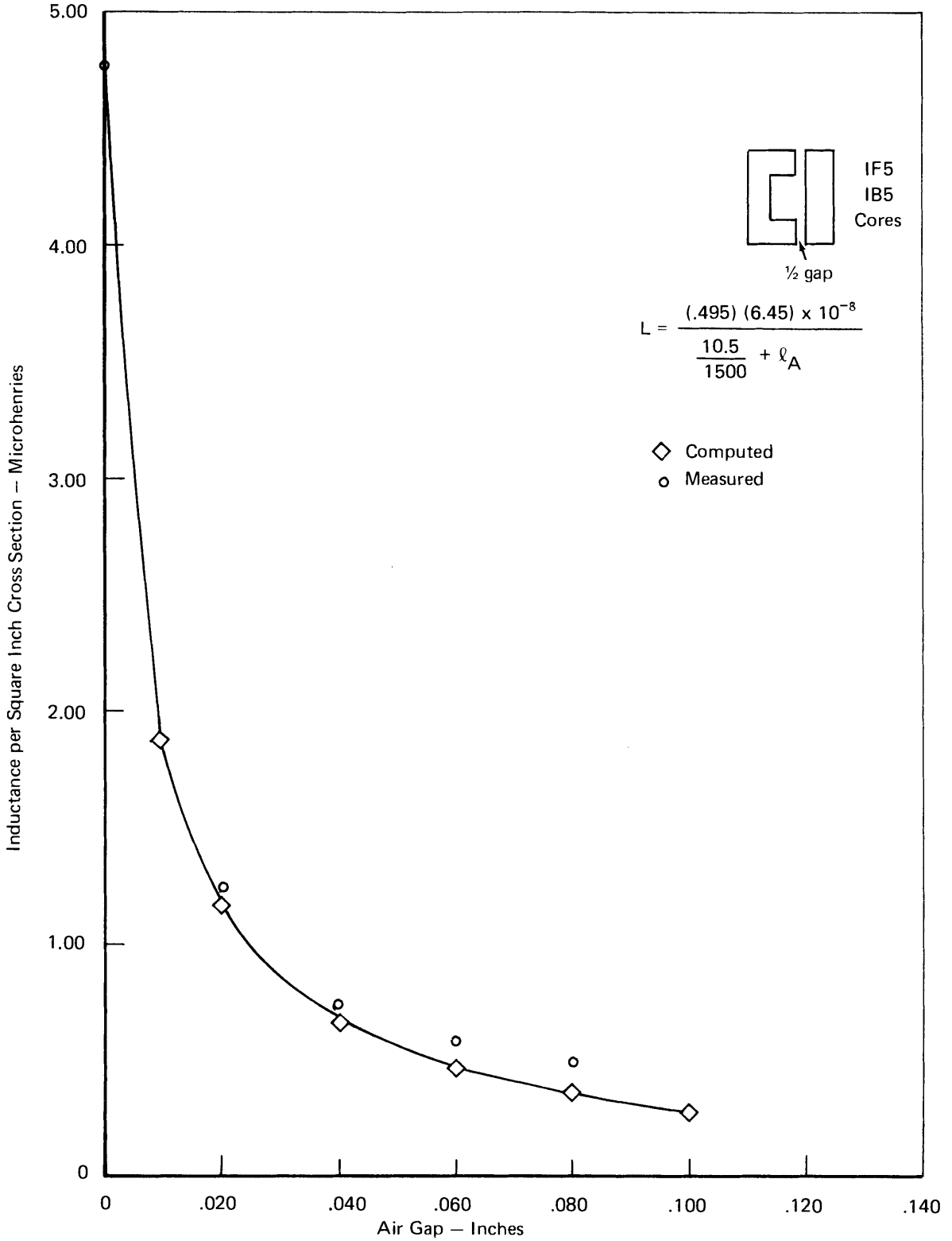

FIGURE 7 SINGLE-TURN INDUCTANCE

1 3C5 FERRITE

3C5 FERRITE

3C5 MATERIAL

A MnZn ferrite for high flux density applications. The losses and permeability are controlled under high flux density, high temperature conditions. This will ensure proper performance in the actual applications.

This 3C5 material is available in the largest standard core configurations produced by Ferroxcube.

Available in:
TOROIDS
E, U & I CORES

3C5 CHARACTERISTICS

Parameters shown are typical values, based upon measurements of a 1" toroid.

Permeability at 25°C, B = 1000 gauss	μ_a	⩾3000
at 100°C, B = 2000 gauss		⩾4000
Losses 100°C, 2000 gauss		160 mW/CM³*
Saturation Flux Density at 25°C, H = 2 oersteds	B_S	3800 gauss*
Coercive Force	H_C	0.2 oersted*
Curie Temperature	T_C	⩾200°C

*Typical value

INITIAL PERMEABILITY (μ_o) vs. FREQUENCY

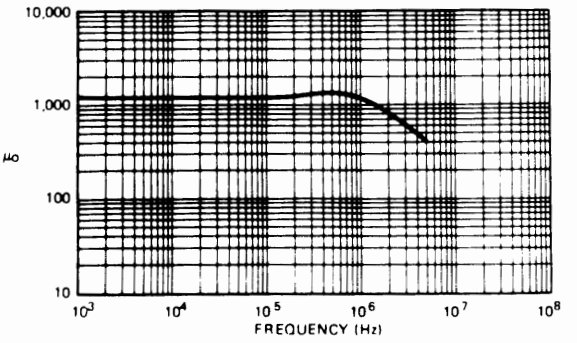

PERMEABILITY (μ_a) vs. FLUX DENSITY ($\hat{B}$)

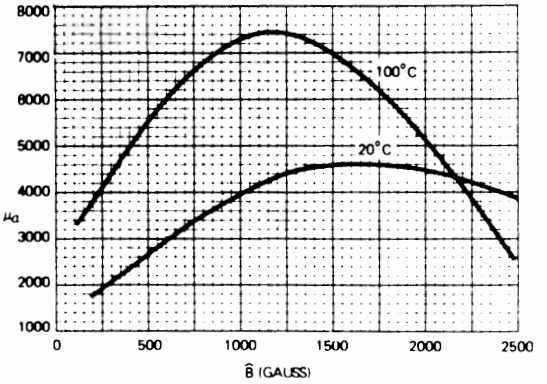

INITIAL PERMEABILITY (μ_o) vs. TEMPERATURE

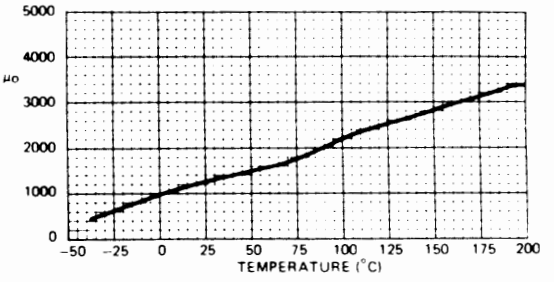

Source: Ferroxcube Corp., *Linear Ferrite Materials & Components Catalogue*

3C5 FERRITE CHARACTERISTIC CURVES

HYSTERESIS CURVE

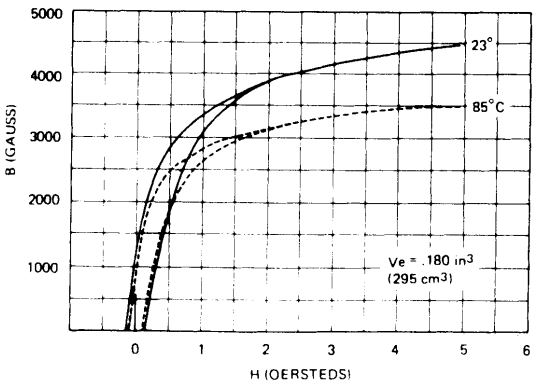

LOSS FACTOR ($\frac{TAN\ \delta}{\mu_o}$) vs. FREQUENCY

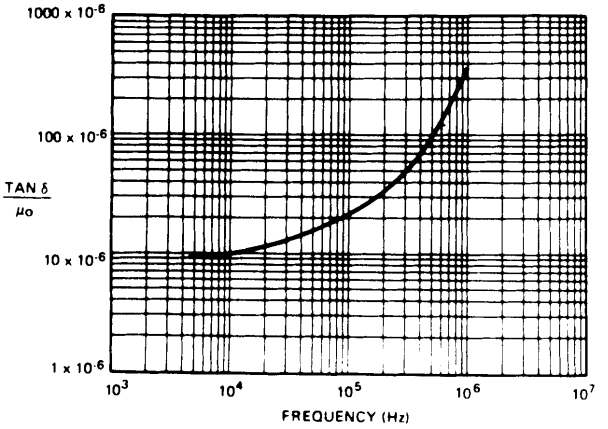

CORE LOSS vs. FLUX DENSITY

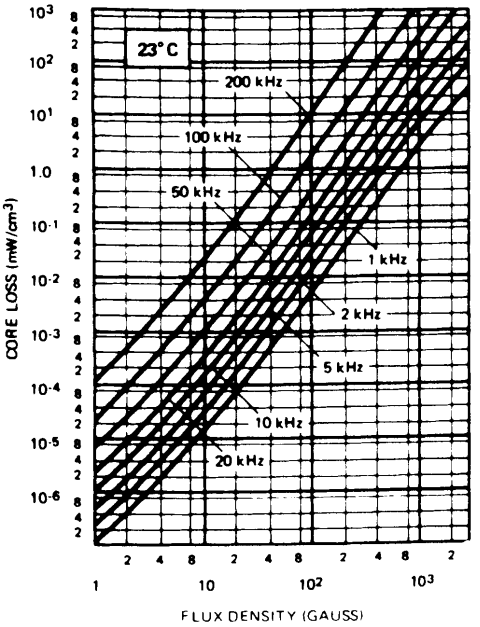

1-9

Source: Ferroxcube Corp., *Linear Ferrite Materials & Components Catalogue*

III. A DIVERSITY METHOD FOR COMBATTING STANDING WAVE NULLS

As discussed in Section F of Chapter I of this Part, unmatched loads placed across the trolley wire/rail transmission line produce reflections that result in standing wave variations in voltage, current, and impedance along the line. In mines, these loads include DC power substations, pumps, motors of haulage vehicles, etc., distributed along the length of the trolley rail network. An example of the voltage and current standing wave patterns produced by a single mismatched load across a lossless line is shown in Figure 1.* The magnitude of the current is greatest when the magnitude of the voltage is smallest, and vice versa; the repetition period of the patterns is a half wave length (approximately one mile at 100 kHz) and the ratio of maximum to minimum magnitudes, VSWR,** (the voltage, or current, standing wave ratio) indicates the degree of mismatch between the load, Z_L, and the line characteristic impedance, Z_o.

Trolley wire carrier phones on mine vehicles are capacitively coupled to the transmission line via the trolley pole drop wire. Consequently, when a vehicle moves into a region containing one of the voltage minima depicted in Figure 1, signal reception may be significantly degraded, and even lost, if the null is deep enough. In those mines where this is a significant and bothersome problem, it may be possible to overcome it in an economical manner; namely, by using modified carrier phones that employ a relatively simple form of switching diversity*** which takes advantage of the fact that the line carrier current and, therefore, the magnetic field are maximum when the voltage is minimum. The method consists of adding a second signal sensor, namely a loop oriented for maximum coupling to the trolley wire magnetic field, and a controlled switch that applies the loop voltage to the carrier phone receiver input whenever the voltage from the drop wire capacitive pick-off falls below a preset reference threshold. The switching process is reversed when the loop voltage falls below the threshold.

Figure 2 depicts in block diagram form the basic elements that need to be added (dashed lines) to the present carrier phones to provide this switching diversity. As shown, the carrier signal, V_1, from one of the sensors is applied to the carrier phone receiver through the diversity switch. In addition to the receiver's normal operations, the amplitude of this signal is measured by means of an envelope detector and then compared with an appropriate preset reference threshold. Whenever the signal, V_1, falls below this threshold, the logic sends a switching control signal to the diversity switch,

---

* References to Figures, Tables, and Equations apply to those in this Chapter unless otherwise noted.

** On a lossy line, the VSWR will eventually decrease to a value of unity as one moves further away from the load, because the reflected wave gradually becomes negligible compared with the incident wave as a result of the line's attenuation.

*** Several types of space, frequency, and polarization diversity reception techniques are commonly used in mobile and point-to-point communications. The switching diversity technique discussed here appears to be the most suited to the mine carrier phone application from the standpoints of simplicity, economy, and performance.

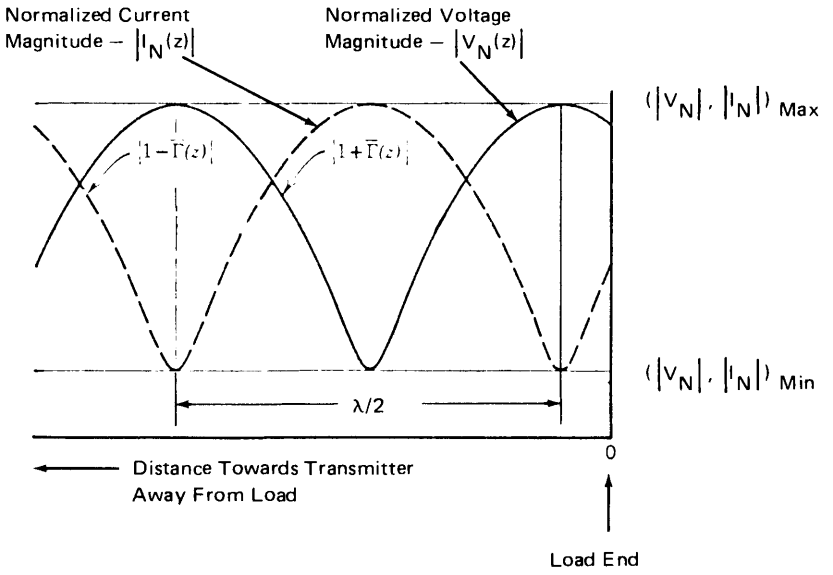

FIGURE 1 SAMPLE VOLTAGE AND CURRENT STANDING WAVE PATTERNS

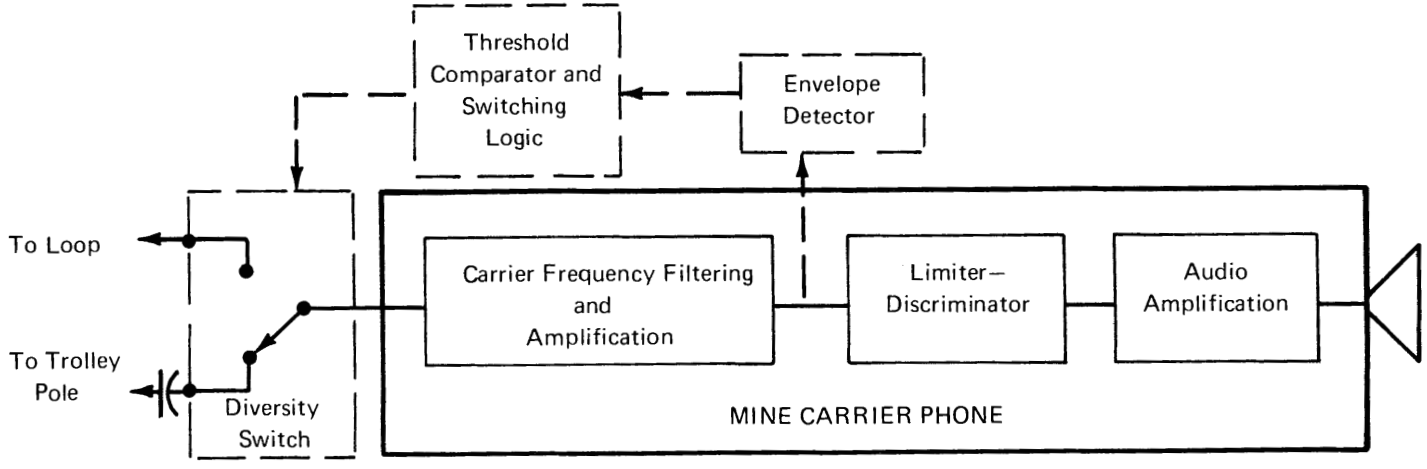

FIGURE 2 CARRIER PHONE WITH MODIFICATIONS FOR SWITCHING DIVERSITY – SIMPLIFIED BLOCK DIAGRAM

which in turn, connects the output, V_2, of the other sensor to the receiver input. Special filtering or integration may also be required in the comparator to avoid false switching caused by impulsive noise transients on the trolley line. This switching process is repeated whenever the applied carrier voltage falls below the threshold.

Preliminary calculations indicate that loop sensors with equivalent cross-sections, NA, of 1-to-10 square meters, should provide loop pick-up voltages well above 10 mv for typical trolley wire carrier currents of about 0.5-to-1 ampere. Although loop orientation for maximum response will be somewhat influenced by the haulage vehicle material and structure, best results should be obtained when the trolley wire lies in, or near to, the plane of the loop. Loops loaded with magnetic material, such as ferrite, should probably be avoided because of the presence of high DC background magnetic fields which may saturate such materials. In fact, a rectangular multi-turn air core loop of heavy construction, attached to the vehicle with the short dimension vertical and the long dimension running the length available on top of the vehicle, may offer the right combination of performance, convenience, and ruggedness.

Further investigation, including experiments, is required to define the most suitable loop sensor size and configuration, and to assess the effectiveness and practicality of the above described switching diversity method for application to mine haulage vehicles for improving transmission as well as reception performance. Finally, the mine carrier phone application may well lend itself to the simplest embodiment of this diversity method, namely, a completely manual switching operation. This possibility arises because of the gradual manner in which the communication performance will be degraded as the haulage vehicle approaches null regions, as opposed to the fast fading phenomena experienced with surface mobile communications at much higher frequencies. In this manual mode, the only modifications required will be associated with the additional loop attached to the vehicle and an appropriate mechanical switch that the vehicle operator can throw when the reception is poor or nonexistent on one of the sensors. In fact, this rudimentary configuration should provide a simple and quick way to check the practical feasibility of this type of diversity in operational mine environments and with currently installed carrier phones on mine haulage vehicles.